www.czasopisma.pan.pl www.journals.pan.pl
Chemical and Process Engineering 2017, 38 (3), 465-475
DOI: 10.1515/cpe-2017-0036

NUMERICAL ANALYSIS OF MOMENTUM TRANSFER PROCESSES IN A MECHANICALLY AGITATED AIR – BIOPHASE – LIQUID SYSTEM

Monika Musiał, Magdalena Cudak, Joanna Karcz*

West Pomeranian University of Technology, Szczecin, Department of Chemical Engineering, al. Piastów 42, 71-065 Szczecin, Poland

The results of numerical computations concerning momentum transfer processes in an air – biophase – liquid system agitated in a bioreactor equipped with baffles and a Smith turbine (CD 6 impeller) are presented in this paper. The effect of sucrose concentration on the distributions of the velocity of the continuous phase, gas hold-up and the size of gas bubbles in the system was analysed. Simulation results were presented in the form of the contours of the analysed magnitudes. The effect of sucrose concentration on the averaged values (i.e. determined on the basis of local values) of gas hold-up and gas bubbles size was evaluated. The results of the numerical computations of gas hold-up were compared with our own experimental data.

Keywords: numerical modelling, momentum transfer, gas – solid – liquid system, bioreactor

1. INTRODUCTION

When straight blades of the Rushton turbine are curved with radius R, the modified high speed impeller can rotate in an agitated vessel in this way that blades push forward on the fluid with their concave or convex parts. The turbine disc impeller with six concave blades is known in literature as the Smith turbine (CD 6 impeller) and is recommended for gas dispersion in the liquid phase. Reduced cavities formed behind the blades compared to those for the Rushton turbine (Bakker, 2000) can be mentioned as the main advantages of the CD 6 impeller. Literature survey on different applications of the turbine impeller with curved blades shows that experimental studies concerning power consumption and mass and heat transfer were carried out mainly by Bielka et al. (2014); Frijlink (1987); Karcz and Kamińska-Borak (1997); Rielly et al. (1992); Sensel et al. (1993); Smith and Katsanevakis (1993); Van't Riet et al. (1976); Warmoeskerken and Smith (1989); Zhengming et al. (1991). Karcz and Kamińska-Brzoska (1994a,b) studied experimentally the influence of the geometrical parameters of the turbine with concave and convex blades on power consumption and heat transfer process in the liquid phase. Gas dispersion in the liquid phase in the agitated vessel equipped with a turbine disc impeller with curved blades was experimentally analysed by Cudak (2011, 2014); Musiał et al. (2015); Rielly et al. (1992); Sensel et al. (1993); Smith and Katsanevakis (1993); Van't Riet et al. (1976); Warmoeskerken and Smith (1989) and Zhengming et al. (1991).

Junker et al. (2000) experimentally examined dual impeller combinations of CD 6 impeller in fermentation vessels. They stated that the use of dual CD 6 impellers and hybrids containing the CD 6 impeller decreases power consumption and increases mass transfer rate in the gas – liquid system compared to results obtained for systems equipped with dual Rushton turbines.

*Corresponding authors, e-mail: Joanna.Karcz@zut.edu.pl

Using CFD simulation, Kharpe and Munshi (2014) carried out a numerical comparison of the Rushton turbine and CD 6 impellers operating in a non-Newtonian fluid agitated in a baffled vessel within the fully turbulent flow regime. Numerical results revealed that the flow field generated by the CD 6 impeller is smaller in magnitude than that for the Rushton turbine. Problems of simulation of gas – liquid hydrodynamics in a baffled agitated vessel with the Rushton turbine were analysed, in detail, by Scargiali et al. (Scargiali et al., 2007). An Eulerian – Eulerian approach was used with the k - ε turbulence model. All bubbles were assumed to be of the same size. The effect of inter-phase forces on the results of simulation was considered. Numerical results were found to be in satisfactory agreement with experimental data.

Recently, a method of multiphase computational fluid dynamics coupled with the population balance method (CFD-PBM) has been successfully used to investigate hydrodynamics and mass transfer in gas-liquid agitated vessels (Gimbun et al., 2009; Musiał et al., 2014; Ranganathan and Sivaraman, 2011). Gimbun et al. (2009) used these methods to analyse scale-up problems for mechanically agitated gas-liquid systems in a vessel equipped with the Rushton turbine or CD 6 impeller. They conducted multiphase simulations using the Eulerian-Eulerian two-fluid model. The authors obtained the local bubble size distribution by solving the PBM using the quadrature methods of moments (QMOM). Devi and Kumar (2011, 2013) applied a CFD method to analyse flow patterns in an agitated vessel equipped with single or double CD 6 impellers. In the case of the single CD 6 impeller, multiple reference frames (MRF) impeller model and realizable k-ε turbulence model were used (Devi and Kumar, 2011). For this case, CFD simulations predicted more turbulent kinetic energy dissipation near the vicinity of CD 6 impeller than for the Rushton turbine. Analysis of the numerical results obtained for the systems of the dual Rushton and CD 6 impellers showed that formation of the merging flow pattern is different in case of CD 6 impellers than in the case of Rushton turbines (Devi and Kumar, 2013).

Results of numerical simulation of hydrodynamics in an agitated vessel equipped with a turbine disc impeller with concave or convex blades make it possible to estimate local changes in the velocity of the fluid flow, therefore it is worth carrying out such computations in order to complete and extend experimental results.

The results of numerical computations concerning momentum transfer processes in an air – biophase – liquid system agitated in a bioreactor equipped with baffles and the Smith turbine (CD 6 impeller) are offered in this paper. The effect of sucrose concentration on velocity distributions in the continuous phase, gas hold-up and the size of gas bubbles in the system were analysed. The results of numerical calculations were compared with our previous experimental results.

2. THE RANGE OF SIMULATIONS

Computations were carried out for a baffled vessel of inner diameter D = 0.288 m. Liquid height in the bioreactor was equal to $H = D$ (Fig. 1a). Four flat baffles of width $B = 0.1D$ were symmetrically arranged on the inner wall of the vessel. A six-bladed CD 6 impeller of diameter $d = 0.33D$ was located on the height $h = 0.33D$ from the flat bottom of the vessel. Blades of the impeller had the following dimensions: length $a = 0.25d$, width $b = 0.2d$ and curvature radius $R = 0.5b$ (Fig. 2). Air was introduced into the bioreactor through a gas sparger in the shape of a ring, located under the impeller in the distance $e = 0.5h$ from the vessel bottom.

A three phase gas – biophase – liquid system was tested experimentally. An aqueous solution of sucrose with the concentration of 2.5, 5 or 10 % mass was used as the liquid phase. The aqueous suspension of yeasts with the concentration of 1 % was applied as the biophase. For the purposes of numerical calculations, the liquid pseudo-phase consisted of the aqueous solution of sucrose and 1% yeast (biophase) was assumed. Air was the dispersed phase. The air flow rate was equal to

V_g = 3.89×10^{-4} m^3/s (w_{og} = 5.97×10 $^{-3}$ m/s; *vvm* = 1.245 (m^3/min)/m^3). Oxygen solubility in the broth was determined experimentally and amounted to 7 mg/dm^3. Oxygen consumption was measured during experiments by means of an oxygen sensor.

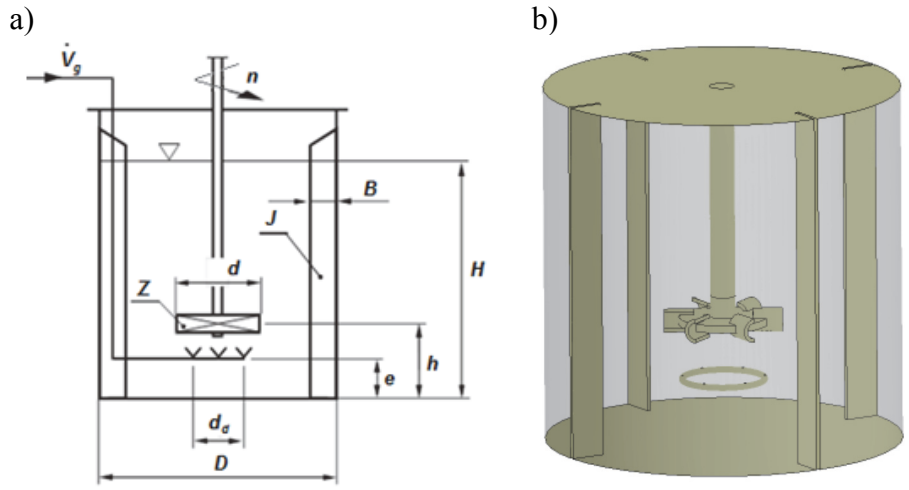

Fig. 1. Geometrical parameters of the agitated vessel

The system containing the aqueous solution of sucrose and yeast suspension showed the properties of a non-Newtonian fluid – shear thinning liquid. Viscosity was measured using a rheometer Haake RT 10. The physical properties of sucrose and yeast suspension were described in detail by Major-Godlewska et al. (Major-Godlewska et al, 2015).

Physical properties of the media, determined experimentally, depended on sucrose concentration and changed within the following ranges: density ρ [kg/m^3] ∈ <1009; 1041>; interfacial tension σ[N/m] ∈ <0.076; 0.086>; viscosity $\eta = k \cdot \gamma^{m-1}$ where k ∈ <0.001183; 0.005241>; m ∈ <0.7129; 0.9699>.

Computations were performed for the impeller speed equal to n = 12 1/s (within the turbulent range of the fluid flow). Experimental studies performed for the physical system considered in this paper showed that below the agitator speed of 8 1/s poor dispersion of the gas in the liquid phase was observed, whereas surface aeration of the liquid was observed above 13 1/s.

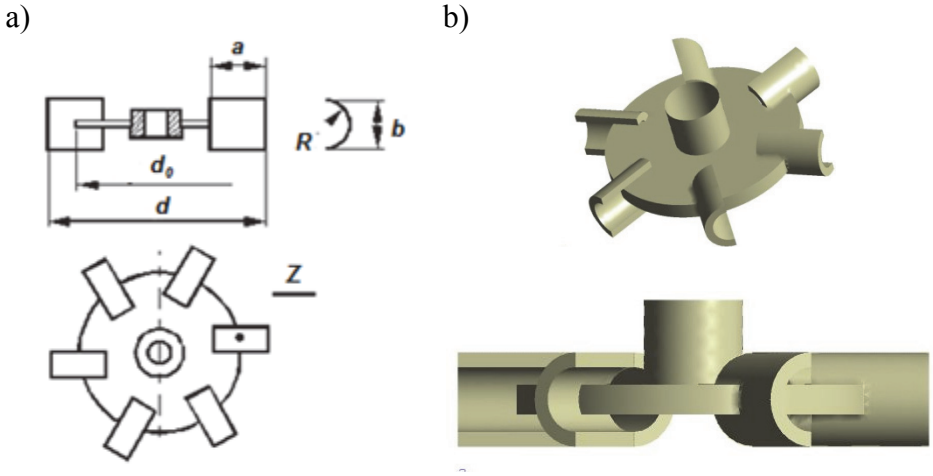

Fig. 2. Geometrical parameters of the CD 6 impeller

Numerical simulations were carried out using ANSYS Workbench and CFX solver version 16.1 (ANSYS, 2013). Geometry of the system was generated using ANSYS Design Modeler. Numerical

grids, created in ANSYS Mesh software, were made for two regions: the impeller-swept region and one for the rest of the bulk zone, in order to use the MRF (Multiple Reference Frames) method. For the geometry of the baffled agitated vessel with a turbine disc impeller with curved blades and the gas sparger, final numerical unstructured meshes consisted of over 920000 tetrahedral elements. Characteristic parameters of the mesh were as follows: a) aspect ratio 1.85; b) element quality 0.84; c) orthogonal quality 0.86. Such values correspond to acceptable quality of the used numerical mesh (ANSYS Inc., 2013).

The Euler-Euler numerical approach was used for simulations. Zero Equation model was used for the modelling of the dispersed phase. Shear Stress Transport (SST) model as the turbulence model and interactions between phases (resistance forces, coalescence and breakage models, turbulent transport) were taken into account in computations (Chung, 2002; Laudner and Spalding, 1974). The breakup model of Luo Svendsen and the coalescence model of Prince-Blanch were used to describe, respectively, breakage and coalescence of gas bubbles. Interphase transfer was determined using *Particle* model. The forces of interphase drag were defined using Schiller-Naumann equation of drag force. To model turbulence transfer between phases the Sato Enhanced Eddy Viscosity correlation was used. Turbulent dispersion force was determined using the Lopez de Bertodano model. The sizes of gas bubbles, divided into ten classes, were modelled by means of the Multiple Size Group Model (MUSIG).

In each simulation the boundary condition on the walls was set at “wall boundary condition”, while on the top of the vessel the boundary condition was set at the outlet with degassing condition in case of gas – liquid system. The gas distributor was modelled as an air inlet with a defined mass flow rate. On the shaft, the boundary condition was set at “rotating wall boundary condition” with the speed equal to n = 12 1/s and with the direction consistent with the direction of impeller rotation. The MRF zone was set as the rotation region with the speed of 12 1/s. Computations were carried out until residuals reached the value of 10^{-4}.

3. RESULTS AND DISCUSSION

The results of numerical simulations are visualized in the form of contour maps. The distributions of liquid velocity, gas hold-up, gas bubble size and kinetic energy of turbulence were shown at three radial inter-sections of the bioreactor (under and above the impeller and at the impeller plane: h/H = 0.26; 0.33; 0.43) (Fig. 3a), as well as at two axial inter-sections (at the baffles plane (0°) and the plane located symmetrically between baffles (45°)) (Fig. 3b).

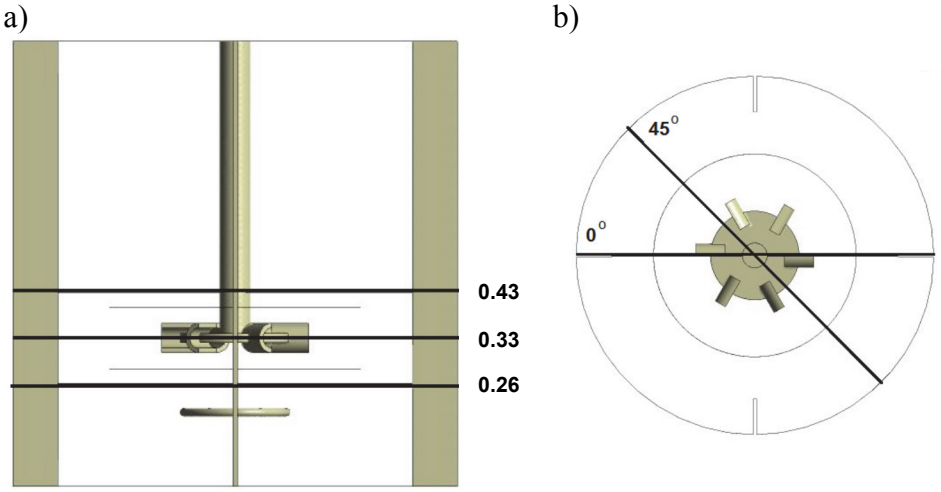

Fig. 3. Inter-sections of the bioreactor: a) axial, b) radial

Axial contours of liquid velocity in the bioreactor, obtained for different concentrations of the sucrose solutions in the liquid phase and two axial inter-sections (at the baffles plane (0°) and the plane located symmetrically between baffles (45°)), are presented in Figs. 4 - 5.

A comparison of the velocity contours in Figs. 4 - 5 shows that the most intensive agitation has taken place in the impeller zone. Liquid velocity behind impeller blades decreases with the increase of the yeast suspension concentration in the bioreactor. Axial contours of the gas hold-up φ, obtained for different sucrose solutions in the liquid phase and two axial inter-sections (at the baffle plane (0°) and the plane located symmetrically between baffles (45°)), are compared in Figs. 6 - 7. More asymmetry of the gas hold – up contours is observed for the axial plane located between baffles (Fig. 7). The highest values of the gas hold-up correspond to the regions located above the impeller. In the zone of the vessel located directly below the impeller gas bubbles are weakly dispersed. However, the dispersion of gas bubbles in the liquid improves when radial distance to the vessel wall in this zone decreases.

Examples of the axial distributions of gas bubble size in the bioreactor equipped with the Smith turbine (CD 6) are presented in Figs. 8 – 9. The smallest diameters of gas bubbles, equal to about 1 mm, correspond to the impeller zone (z/H = 0.33). Gas bubble diameter increases in the direction of the free surface of the liquid in the bioreactor. The most symmetrical distribution of gas bubble sizes was obtained for a physical system in which sucrose concentration in the liquid was equal to 5 % mass (Fig.8b, 9b).

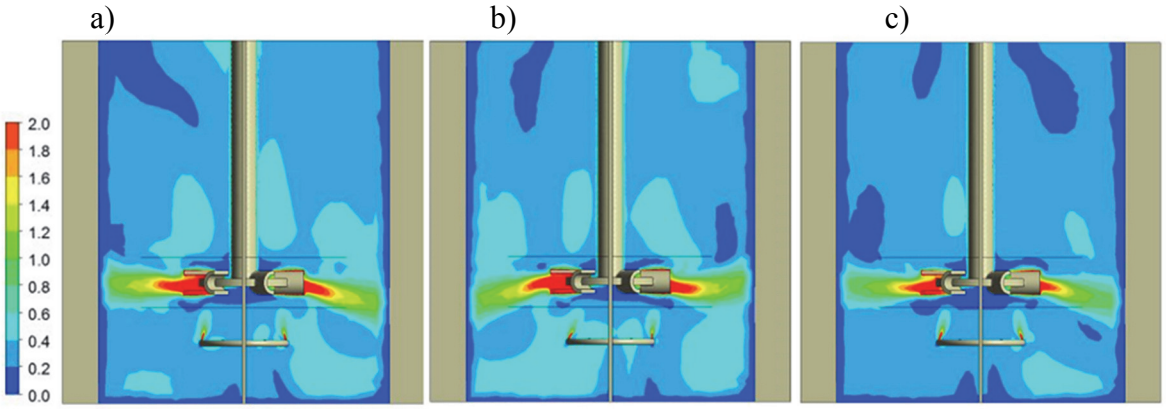

Fig. 4. Axial contours of liquid velocity at baffle plane (0°): a) air – 1% yeast suspension – 2.5% aqueous solution of sucrose, b) air – 1% yeast suspension – 5% aqueous solution of sucrose, c) air – 1% yeast suspension – 10% aqueous solution of sucrose

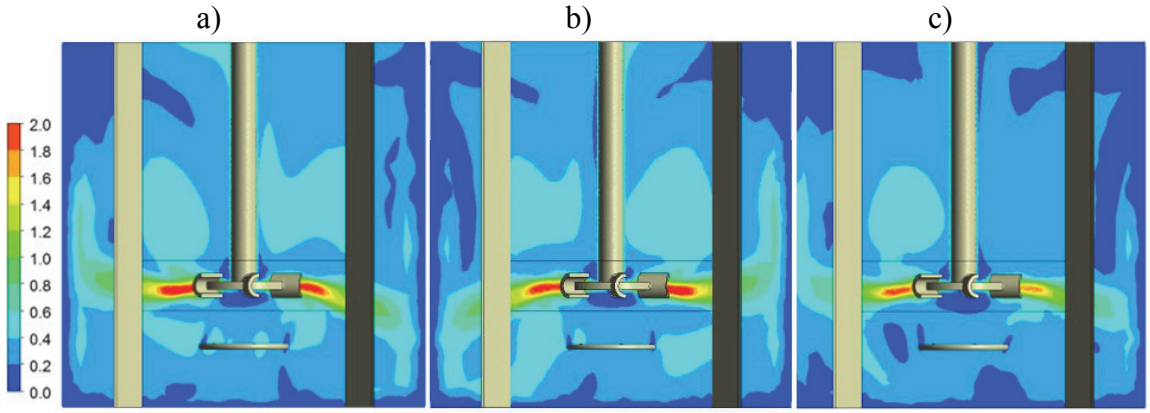

Fig. 5. Axial contours of liquid velocity at the plane located symmetrically between baffles (45°): a) air – 1% yeast suspension – 2.5% aqueous solution of sucrose, b) air – 1% yeast suspension – 5% aqueous solution of sucrose, c) air – 1% yeast suspension – 10% aqueous solution of sucrose

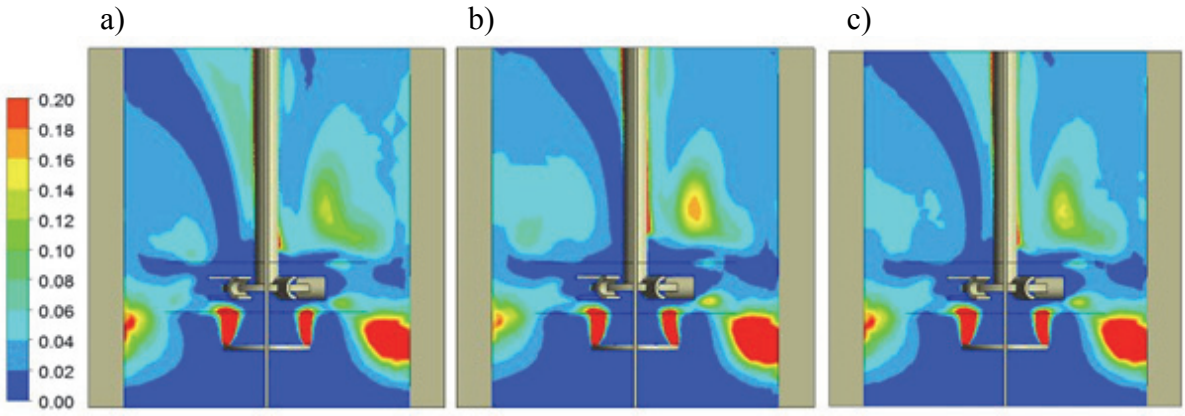

Fig. 6. Axial contours of the gas hold-up φ at baffle plane (0°): a) air – 1% yeast suspension – 2.5% aqueous solution of sucrose, b) air – 1% yeast suspension – 5% aqueous solution of sucrose, c) air – 1% yeast suspension – 10% aqueous solution of sucrose

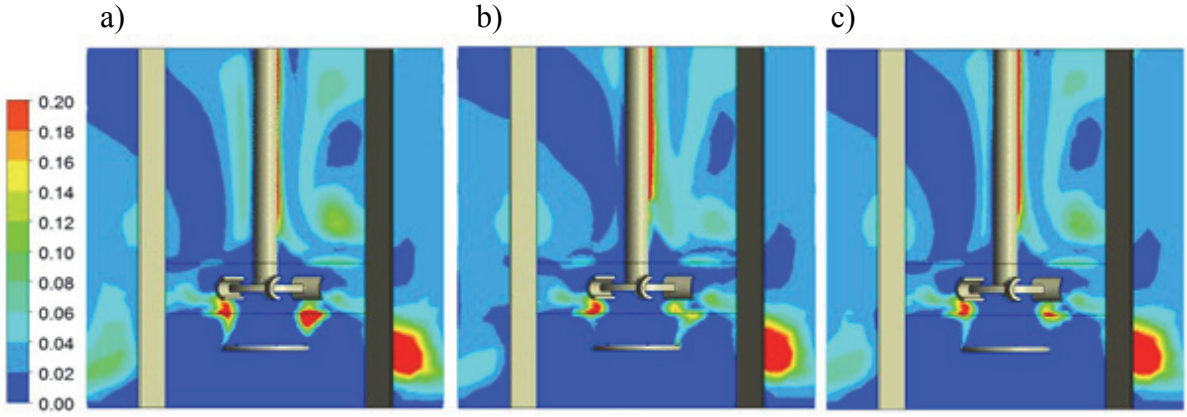

Fig. 7. Axial contours of the gas hold-up φ at the plane located symmetrically between baffles (45°): a) air – 1% yeast suspension – 2.5% aqueous solution of sucrose, b) air – 1% yeast suspension – 5% aqueous solution of sucrose, c) air – 1% yeast suspension – 10% aqueous solution of sucrose

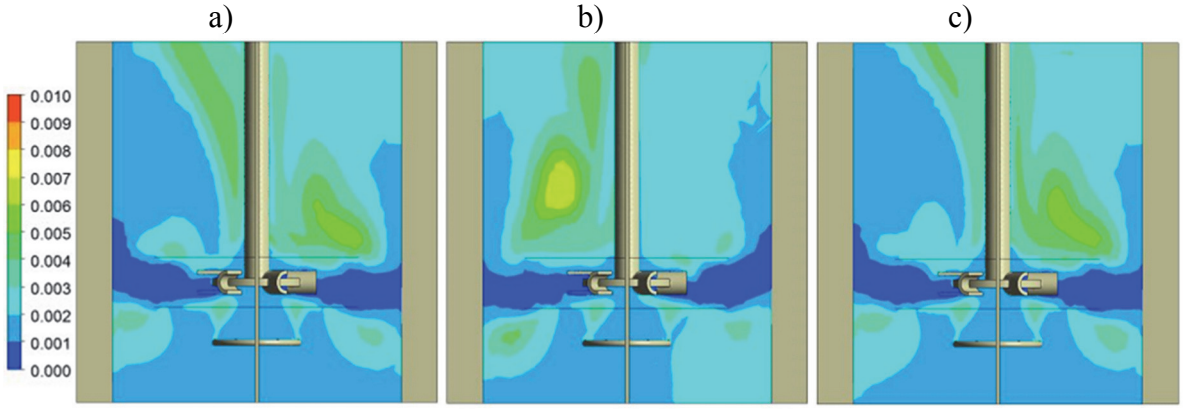

Fig. 8. Axial contours of the gas bubbles size at baffle plane (0°): a) air – 1% yeast suspension – 2.5% aqueous solution of sucrose, b) air – 1% yeast suspension – 5% aqueous solution of sucrose, c) air – 1% yeast suspension – 10% aqueous solution of sucrose

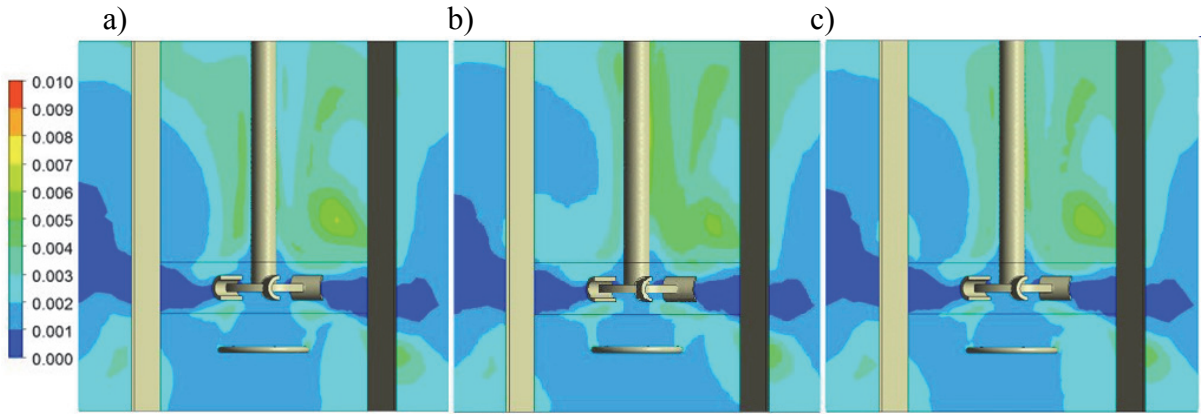

Fig. 9. Axial contours of the gas bubbles size at the plane located symmetrically between baffles (45°): a) air – 1% yeast suspension – 2.5% aqueous solution of sucrose, b) air – 1% yeast suspension – 5% aqueous solution of sucrose, c) air – 1% yeast suspension – 10% aqueous solution of sucrose

Distributions obtained in numerical calculations depend on the level of the agitator speed n, gas flow rate V_g and physical properties of the gas – liquid pseudo-phase (especially viscosity), as well as on the interaction between those parameters. Certain asymmetry of hydrodynamic distributions is observed in Figs. 4 - 9. These results can be explained as follows: the plane of the axial cross-section divides the vessel in this way that the position of both opposite curved blades of the impeller in this plane is not identical.

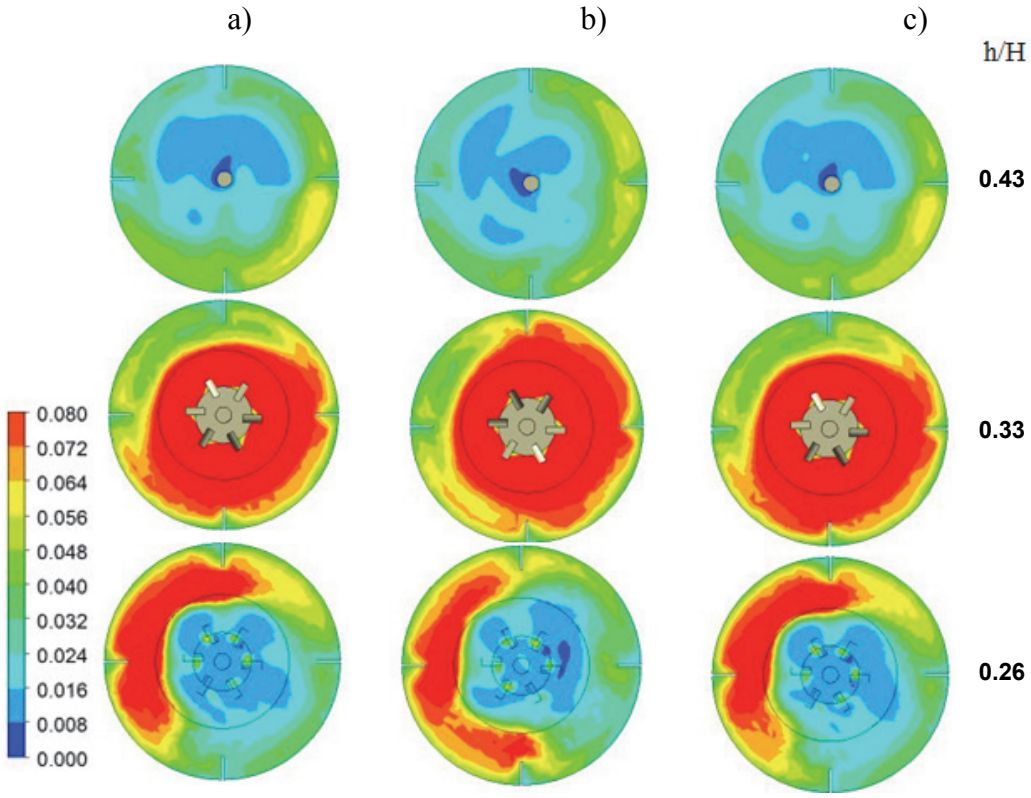

Fig. 10. Radial contours of turbulence kinetic energy k a) air – 1% yeast suspension – 2.5% aqueous solution of sucrose, b) air – 1% yeast suspension – 5% aqueous solution of sucrose, c) air – 1% yeast suspension – 10% aqueous solution of sucrose

At one axial half cross-section, rotation of the impeller makes the fluid flow round the convex side of the blade, whereas the concave side of the opposite blade in this plane is passed by the fluid at the

second axial half cross-section. Therefore, the local values of the analysed magnitudes on the right and left sides of the impeller shaft in this plane correspond to opposite points of the circulation loop, resulting from the convex or concave curvature of impeller blades. For this reason, certain asymmetry of hydrodynamic distributions can be justified. Strictly symmetrical distributions are characteristic only for flat blades of the impeller (Rushton turbine), where both opposite blades at the axial plane have an identical shape. The contours of the turbulence kinetic energy k and dissipation of turbulence kinetic energy ε for three levels of the dimensionless axial coordinate h/H equal to 0.26 (under impeller), 0.33 (level of the impeller disc) and 0.43 (above impeller) are shown in Figs. 10 - 11. On the basis of the performed simulations, an insignificant effect of sucrose concentration in the liquid phase was observed only in the values of turbulence kinetic energy k and dissipation of turbulence kinetic energy ε. The highest values of both k and ε corresponded to the level of the impeller height. In all the analysed cases, an asymmetry in the distributions of turbulence kinetic energy k was observed (Fig. 10).

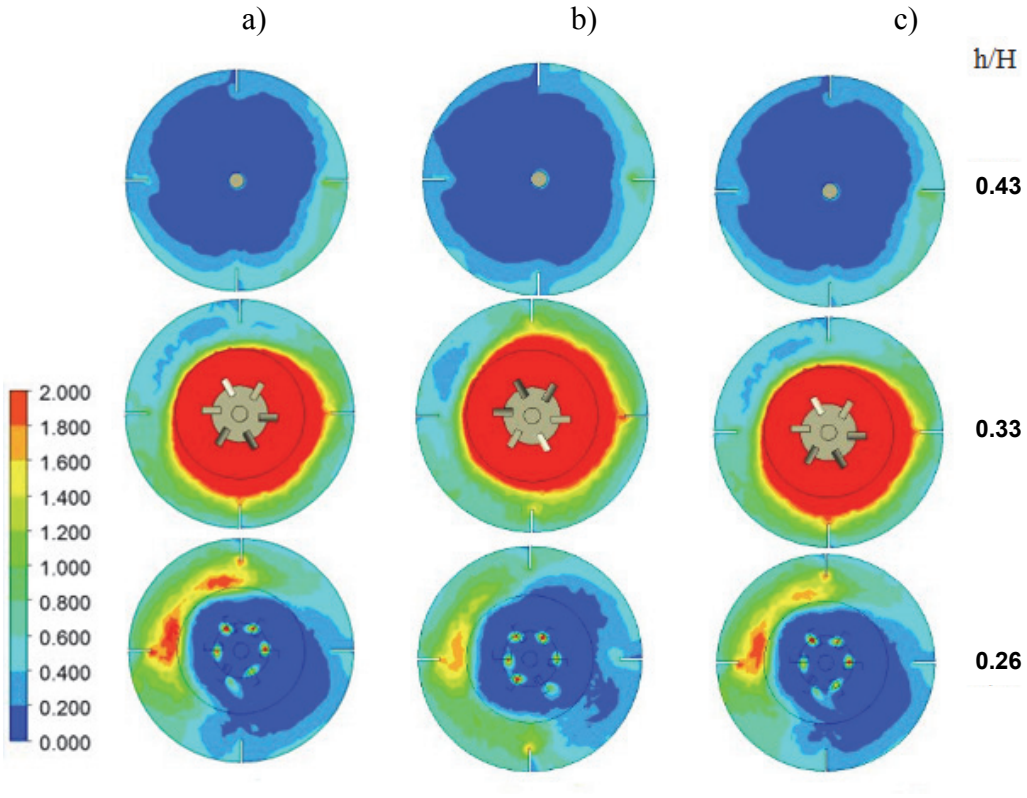

Fig. 11. Radial contours of dissipation of turbulence kinetic energy: a) air – 1% yeast suspension – 2.5% aqueous solution of sucrose, b) air – 1% yeast suspension – 5% aqueous solution of sucrose, c) air – 1% yeast suspension – 10% aqueous solution of sucrose

It is probably caused by disadvantageous hydrodynamic interaction between planar baffles and concave blades of the turbine impeller. The highest differences between values of the turbulence kinetic energy k exist in the region below the impeller in the bioreactor (h/H = 0.26, Fig. 10). The contours of energy dissipation ε obtained for both levels of the dimensionless axial coordinate h/H equal to 0.33 (level of the impeller disc) and 0.43 (above impeller) are more symmetrical than the contours for level h/H = 0.26 (Fig. 11).

Local values of the analysed parameters were numerically integrated for each plane of the bioreactor. Averaged values of the liquid velocity w, size of gas bubbles d_b, turbulence kinetic energy k and dissipation of turbulence kinetic energy ε are compared in Table 1 for different physical systems. A comparison between the averaged values of gas hold-up φ, determined numerically and our

experimental values (Musiał et al., 2015), is given in Table 2. Relative mean errors collected in Table 2 show sufficient agreement between both numerical and experimental values of the gas hold-up.

Table 1. Comparison of the averaged values of liquid velocity w, size d_b of gas bubbles, turbulence kinetic energy k and the dissipation of turbulence kinetic energy ε for different physical systems

	air – 1% yeast suspension – 2.5% aqueous solution of sucrose	air – 1% yeast suspension – 5% aqueous solution of sucrose	air – 1% yeast suspension – 10% aqueous solution of sucrose
w, m/s	0.629	0.625	0.624
d_b, m	1.975×10^{-3}	1.946×10^{-3}	2.057×10^{-3}
k, m^2/s^2	6.321×10^{-2}	6.301×10^{-2}	6.502×10^{-2}
ε, m^2/s^3	88.18	88.08	93.14

Table 2. Comparison of averaged values of gas hold-up φ

System	φ_{num}	φ_{exp}	$\pm\Delta$, %
air – 1% yeast suspension – 2.5% aqueous solution of sucrose	0.109	0.080	26.6
air – 1% yeast suspension – 5% aqueous solution of sucrose	0.101	0.083	17.8
air – 1% yeast suspension – 10% aqueous solution of sucrose	0.109	0.095	12.8

4. CONCLUSIONS

The results of the numerical simulations of hydrodynamics in the agitated vessel equipped with CD 6 impeller (Smith turbine) show that within the range of computations performed for a three phase gas – biophase – liquid system:

- The local values of liquid velocity decrease with the increase of biophase concentration in the fluid,
- The distributions of gas hold–up and gas bubble size slightly depend only on the concentration of sucrose in the liquid phase.

SYMBOLS

a length of the impeller blade, m
B width of baffle, m
b width of the impeller blade, m
D vessel diameter, m
d impeller diameter, m
d_b gas bubble size, m
d_d sparger diameter, m
d_o disc diameter, m
e clearance between gas sparger and vessel bottom, m
H liquid height in the agitated vessel, m
h distance of the impeller from the vessel bottom, m
J number of baffles
k consistency index
k turbulence kinetic energy, m^2/s^2
m flow index

n	impeller speed, 1/s
R	radius of the blade curvature, m
vvm	volumetric gas flow rate, $(m^3/min)/m^3$
V_g	gas flow rate, m^3/s
w	averaged liquid velocity, m/s
w_{og}	superficial gas velocity, m/s
Z	number of impeller blades
z	axial coordinate, m

Greek symbols

ε	dissipation of turbulence kinetic energy, m^2/s^3
φ	gas hold-up
η	dynamic viscosity of the liquid, Pas
ρ	liquid density, kg/m^3
σ	interfacial tension, N/m

REFERENCES

ANSYS CFX-Solver Theory Guide, Release 15.0, ANSYS, Inc, November 2013.

Bakker A., *The Online CFM Book 2000*. Available at: www.bakker.org/cfm.

Bielka I., Cudak M., Karcz J., 2014. Local heat transfer process for a gas-liquid system in a wall region of an agitated vessel equipped with the system of CD6-RT impellers. *Ind. Eng. Chem. Res*., 53, 42, 16539-16549. DOI: 10.1021/ie503003t.

Chung T.J., 2002. *Computational Fluid Dynamics*. Cambridge Univ. Press.

Cudak M., 2011. Process characteristics for the mechanically agitated gas-liquid systems in the turbulent fluid flow. *Przem. Chem.*, 90, 9, 1000-1004 (in Polish).

Cudak M., 2014. Hydrodynamic characteristics of mechanically agitated air – aqueous sucrose solutions. *Chem. Process Eng*., 35, 1, 97-107. DOI: 10.2478/cpe-2014-0007.

Devi T.T., Kumar B., 2013. Comparison of flow patterns of dual Rushton and CD-6 impellers. *Theor. Found. Chem. Eng.*, 47, 4, 344-355. DOI: 10.1134/S0040570513040210.

Devi T.T., Kumar B., 2011. Analyzing flow hydrodynamics in stirred tank with CD-6 and Rushton impeller. *Int. Rev. Chem. Eng.*, 3, 1, 440-448.

Frijlink J.J., 1987. Roerders in begaste Suspensions. *i^2 – Prozesstechnologie*, 9, 47-51.

Gimbun J., Rielly C.D., Nagy Z.K., 2009. Modelling of mass transfer in gas-liquid stirred tanks agitated by Rushton turbine and CD 6 impeller: A scale-up study. *Chem. Eng. Res. Des.*, 87, 437-451. DOI: 10.1016/j.cherd.2008.12.017.

Junker H.J., Mann Z., Hunt G., 2000. Retrofit of CD-6 (Smith) impeller in fermentation vessels. *Appl. Biochem. Biotechnol*., 89, 1, 67-83. DOI: 10.1385/ABAB:89:1:6.

Karcz J., Kamińska-Brzoska J., 1994. Experimental studies of the influence of the blade curvature of a disc turbine on power consumption. *Inż. Chem. Proc*., 15, 3, 371-378.

Karcz J., Kamińska-Brzoska J., 1994. Heat transfer in a jacketed stirred tank equipped with baffles and concave disc impeller. *8th European Conference on Mixing*, *ICHEME Symposium Series*, 136, 449-456. Cambridge, 21-23.09.1994.

Karcz J., Kamińska-Borak J., 1997. An effect of stirred tank geometry on heat transfer efficiency – Studies for concave disc turbine. *9th European Conference on Mixing*, *Recent Progres en Genie des Procedes*, 11, 51, 265-272. Paris 18-21.03. 1997.

Khapre A., Munshi B., 2014. Numerical comparison of Rushton turbine and CD-6 impeller in non-Newtonian fluid stirred tank. *International Scholarly Scientific Research Innovation*, 8, 11, 1260-1267. Available at: scholar.waset.org/1999.2/5555526.

Laudner B.E., Spalding J.L., 1974. The numerical computation of turbulent flows. *Comput. Methods Appl. Mech. Eng.*, 3, 269-289. DOI: 10.1016/0045-7825(74)90029-2.

Major-Godlewska M., Bitenc M., Karcz J., 2015. Experimental analysis of an effect of the nutrient type and its concentration on the rheological properties of the baker's yeast suspensions. *Polish J. Chem. Technol.*, 17, 3, 110-117. DOI: 10.515/pjct-2015-0058.

Musiał M., Karcz J., Cudak M., 2014. Use of CFD metod for analysis of hydrodynamics in a baffled agitated vessel with CD 6 impeller. *Przem. Chem*., 93, 9, 1599-1603 (in Polish).

Musiał M., Cudak M., Karcz J., 2015. Gas hold-up for gas-liquid-biophase systems in the bioreactor with CD 6 impeller. *Inż. i Ap. Chem*., 54, 4, 182-183 (in Polish).

Ranganathan P., Sivaraman S., 2011. Investigations on hydrodynamics and mass transfer in gas–liquid stirred reactor using computational fluid dynamics. *Chem. Eng. Sci.,* 66, 3108-312 4. DOI: 10.1016/j.ces.2011.03.007.

Rielly C.D., Evans G. M., Davidson J.F., Carpenter K.J., 1992. Effect vessel scale-up on the hydrodynamics of a self-aerating concave blade impeller. *Chem. Eng. Sci.*, 47, 13/14, 3395-3402. DOI: 10.1016/0009-2509(92)85050-L.

Scargiali F., D'Orazio A., Grisafi F., Brucato A., 2007. Modelling and simulation of gas-liquid hydrodynamics in mechanically stirred tanks. *Chem. Eng. Res. Des.*, 85(A5), 637–646. DOI: 10.1205/cherd06243.

Sensel M.E., Meyers K.J., Fasano J.B., 1993. Gas dispersion at high aeration rates in low to moderately viscous Newtonian liquids. *Process Mixing: Chem. Biochem. App., Part II, AIChE Sym*p. *Ser.,* 89, 293, 76-81.

Singh H., Fletcher D. F., Nijdam J. J., 2011. An assessment of different turbulence models for predicting flow in a baffled tank stirred with a Rushton turbine. *Chem. Eng. Sci.*, 66, 5976-5988. DOI: 10.1016/j.ces.2011.08.018.

Smith J.M., Katsanevakis A.N., 1993. Impeller power demand in mechanically agitated boiling systems. *Chem. Eng. Res. Des.*, 71, Part A, 145-152.

Van't Riet K., Boom J.M., Smith J.M., 1976. Power consumption impeller coalescence and recirculation in aerated vessels. *Trans. Inst. Chem. Eng.*, 54, 124-131.

Warmoeskerken M.M.C.G., Smith J.M., 1989. The hollow blade agitator for dispersion and mass transfer. *Chem. Eng. Res. Des*., 67, 193-198.

Zhengming G., Yingchen W., Yanmin Z., Litian S., 1991. Study on gas-liquid mass transfer characteristics in an agitated vessel. Part II. The effects of geometric parameters of an agitated tank on the volumetric mass transfer coefficient. *7th European Conference on Mixing*, Part II, Brugge, Belgium, 18-20.09.1991, 315-320.

Received 10 October 2016
Received in revised form 28 June 2017
Accepted 29 July 2017